Part E : Theory of supernova light curves and spectra

Anders Jerkstrand
Stockholm University

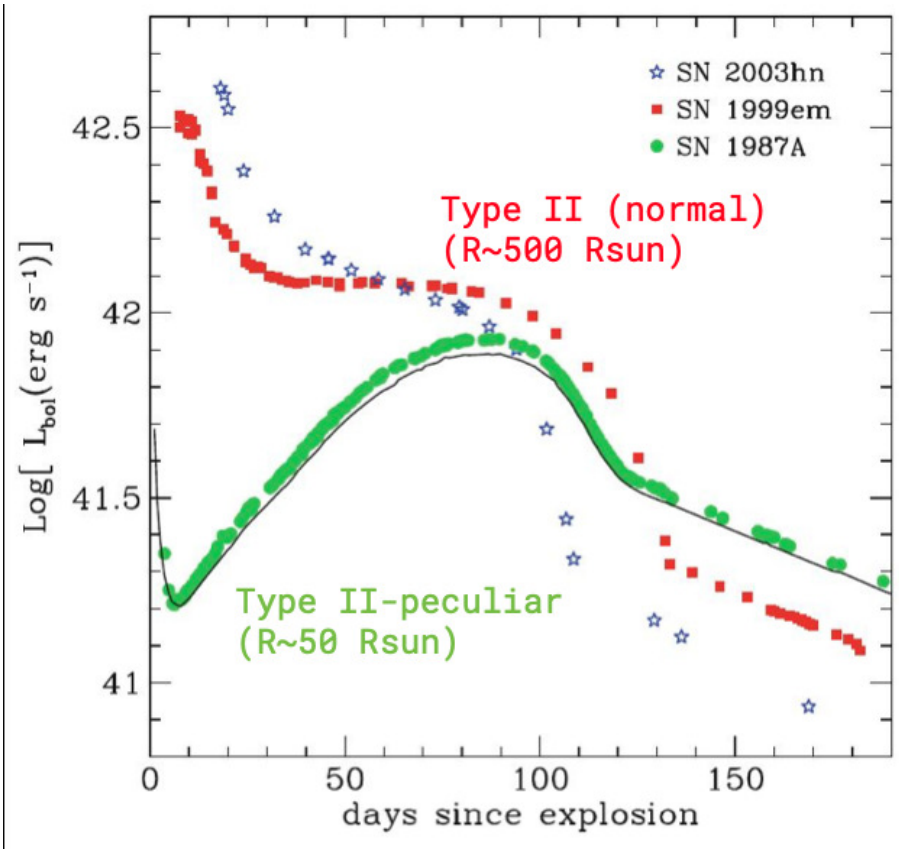

Contents

1 Conditions in the exploding star

A CCSN explosion deposits an energy $E_{dep} \sim 10^{51}$ erg in the inner layers of the collapsing star. This energy is spread to the whole star by a shock wave propagating outwards with $v_{shock} \sim 10^4$ km s^{-1}. It reaches the surface after a time $t_{surf} = R_0/v_{shock}$, where R_0 is the stellar progenitor radius. We can estimate t_{surf} ∼1 minute for the most compact progenitors (WR stars, bare He cores, $R_0 \sim 1\ R_\odot$), and t_{surf} ∼1 day for the most extended ones (RSGs, $R_0 \sim 500\ R_\odot$). The shock breakout begins the light display.

Equipartition. The shocked layers are both accelerated and heated. In

the limit of **strong shocks** ($v_{shock} \gg v_{sound}$), one can show that radiation-dominated gas fulfills equipartition:

$$E^0_{int} = E^0_{kin} = \frac{1}{2} E_{dep} \tag{1}$$

That is, in the shock wake, energy is equally divided between internal energy and bulk kinetic energy. This limit is a good approximation here because $v_{sound} \sim 10$ km s^{-1} in the star, much lower than the shock speed.

The first law of thermodynamics states that *"the change in internal energy in a volume equals the energy deposited, minus the net energy transported out of the volume, minus the work done ("pdV")"*. For a moving gas we write this law most easily on Lagrangian form, with m as the independent variable rather than radius r:

$$\frac{\delta u(m,t)}{\delta t} = s(m,t) - \frac{\partial l(m,t)}{\partial m} - p(m,t) \frac{\partial \left(1/\rho(m,t)\right)}{\partial t} \tag{2}$$

Here u is the internal energy per unit mass (erg g^{-1}), s is the energy deposition rate (e.g. by radioactivity) per unit mass and time (erg s^{-1} g^{-1}), l is the luminosity (erg s^{-1}), p is the pressure (barye =dyne cm^{-2} = erg cm^{-3}), and ρ is the density (g cm^{-3}).

Energy density u**.** The internal energy consists of three main parts:

1) Kinetic motions of particles, for a monoatomic gas $u_{kin} = n \times \frac{3}{2} kT/\rho = \frac{3}{2} kT/\left(Am_p\right)$, where A is the atomic weight.
2) Radiation field energy, which under optically thick equilibrium conditions is $u_{rad} = aT^4/\rho$, where a is the radiation constant $a = 7.56 \times 10^{-15}$ erg cm^{-3} K^{-4}.
3) Potential energy in excited and/or ionized states, $u_{pot} = \rho^{-1} \sum_{i=1}^{N_{states}} n_i E_i$, where n_i is the number density of state i and E_i its energy.

In SNe in the early phases after the shock has passed, radiation energy typically dominates so we can take $\boxed{u \approx u_{rad}}$.

Pressure. The pressure p can be expressed in terms of T and ρ by an equation of state, which for a radiation-dominated gas depends only on T:

$$p = \frac{1}{3} aT^4 = \frac{1}{3} u_{rad} \rho \tag{3}$$

We will return later to the terms for radiation transport ($\frac{\partial l(m,t)}{\partial m}$) and energy deposition ($s(m,t)$) in Eq. 2. If we assume that both of these are unimportant, we get the adiabatic limit of the first law of thermodynamics as follows:

$$\frac{4aT^3 \dot{T}}{\rho} + aT^4 \dot{\left(\frac{1}{\rho}\right)} = \frac{1}{3} aT^4 \dot{\left(\frac{1}{\rho}\right)} \tag{4}$$

giving

$$\frac{4\dot{T}}{T} - \frac{\dot{\rho}}{\rho} = \frac{1}{3}\frac{\dot{\rho}}{\rho} \tag{5}$$

or

$$\frac{\dot{T}}{T} = \frac{1}{3}\frac{\dot{\rho}}{\rho} \tag{6}$$

Because $\dot{\rho}/\rho = -3\dot{r}/r$, we get

$$\frac{\dot{T}}{T} = -\frac{\dot{r}}{r} \tag{7}$$

which has solution

$$\boxed{T = T_0\,(r/r_0)^{-1}} \tag{8}$$

This tells us that the temperature in a shell evolves as the inverse of the radius of the shell as it expands.

Homologous expansion. Quite soon the material reaches free-coasting trajectories (velocity $v \approx$ constant). After some further time, the layers have expanded so far from their starting positions that $r \approx vt$ holds, this is called homology. Then, denoting the beginning of that phase by t_0, $r/r_0 = t/t_0$ and then Eq. 8 becomes

$$T = T_0 \left(\frac{t}{t_0}\right)^{-1} \tag{9}$$

From the point of homology temperature then evolves with the inverse of time. We will make use of this result later when we estimate the SN brightness.

2 Light curve duration

Let λ_{mfp} be the mean-free-path, the typical length photons travel before interacting with matter. We have $\lambda_{mfp} = 1/(\kappa\rho)$, where κ is the opacity (cm^2 g^{-1}). The time between interactions is then λ_{mfp}/c. If N is the required number of scatterings to escape the nebula, the total diffusion time is $t_{diff} = N\lambda_{mfp}/c$. One can show that $N \approx \chi\tau^2$ where $\tau = R/\lambda_{mfp}$ is the optical depth, where we let R denote the outer radius of the expanding nebula (velocity v_{max}). Here χ is a parameter of order unity to allow for choosing photons to start at the centre, at $R/2$, etc. Then

$$t_{diff}(t) = \frac{\chi R(t)^2 \kappa(t)\rho(t)}{c} \tag{10}$$

Using homology ($R(t) = v_{max}t$) and taking a uniform sphere density relation $\rho \approx M/(4\pi/3R^3)$, we get

$$t_{diff}(t) = \frac{3\chi}{4\pi}\frac{\kappa(t)M}{v_{max}tc} \tag{11}$$

Using $E = 3/10 M v_{max}^2$ (uniform sphere case), and finally equating $t_{diff}(\Delta t) = \Delta t$, where Δt is the characteristic duration of the diffusion light curve, we get

$$\boxed{\Delta t = 20\text{d } \chi^{1/2} E_{51}^{-1/4} M_{M_\odot}^{3/4} \kappa_{0.2}^{1/2}} \tag{12}$$

where $E_{51} = E/10^{51}$ erg, $M_{M_\odot} = M/1\ M_\odot$, and $\kappa_{0.2} = \kappa/0.2$ cm^{2}g^{-1}. If ionization can be maintained so that $\kappa_{0.2}$ stays close to unity (0.2 is the value of electron scattering opacity for all fully ionized elements except H which has 0.4), we would therefore expect 10^{51} erg explosions of stars from $1 - 10\ M_\odot$ to display a diffusion-type light curve over $\sim\ 1 - 4$ months.

That the SN diffuses until $t_{diff}(t) = t$ can be shown from numeric simulations, but also be qualitatively understood. If $t_{diff} \ll t$ radiation can immediately escape, the diffusion phase is over and the LC is declining as the internal energy is rapidly radiated away. If $t_{diff} \gg t$ the radiation is still trapped and thus diffusion still ongoing. The transition must come when the two time scales cross over.

Although a simplistic derivation, the *scalings* (the exponents) in Eq. 12 turn out to be quite accurate compared to sophisticated numeric simulations of SN light curves. The weak sensitivity to E suggests that one should be able to estimate $M \times \kappa^{2/3} \propto \Delta t^{4/3} E^{1/3}$ quite accurately from the observed duration of the LC (uncertainty in E has minor impact so having a rough estimate of this can be sufficient).

2.1 Type IIP SNe : considering recombination

The behaviour of Type IIP SNe is somewhat more complex due to strong changes of opacity with time in the ejecta - opacity was assumed constant in the treatment above. When the temperature in a layer reaches the H recombination temperature ($T_{rec} \sim 6000$ K), the opacity drops to almost zero as other opacities than electron scattering are low, and the internal energy in that shell is therefore quickly released. Let us try another approach not relying on opacity. The luminosity is, taking $T_{phot} \approx T_{rec}$ as we know once layers recombine there is almost no opacity outside that layer and thus it should be close to the photosphere:

$$L(t) = 4\pi R_{phot}(t)^2 \sigma T_{rec}^4 \tag{13}$$

If one takes $R_{phot}(t) \approx$ constant $\approx v_{max} \times \frac{\Delta t_{IIP}}{2}$ this becomes

$$L(t) = \pi v_{max}^2 \Delta t_{IIP}^2 \sigma T_{rec}^4 \tag{14}$$

On the other hand, if we say that luminosity should equal a characteristic value of the internal energy, which we take at $\Delta t_{IIP}/2$, over the light curve duration time Δt_{IIP}, then (note that total energy E_{tot} evolves also as t^{-1} as it is $V \times aT^4 \propto t^3 t^{-4}$),

$$L \approx \frac{E_{int}(t = \Delta t_{IIP}/2)}{\Delta t_{IIP}} = \frac{\frac{E}{2} \frac{R_0}{v_{max} \Delta t_{IIP}/2}}{\Delta t_{IIP}} \tag{15}$$

Combining these two expressions to eliminate L we get (letting $M_{10} = M/\left(10\ M_{\odot}\right)$)

$$\boxed{\Delta t_{IIP} = 80\mathrm{d}\ E_{51}^{-1/8} R_{0,500}^{1/4} M_{10}^{3/8}} \tag{16}$$

Here $\sigma = 5.67 \times 10^{-5}$ erg cm^{-2} s^{-1} K^{-4} is the Stefan-Boltzmann constant and $R_{0,500} = R_0/500\ R_{\odot}, M_{10} = M/\left(10\ M_{\odot}\right)$. In this framework

- The dependency on E and M in Eq. 16 is weaker than in Eq 12. This weakness means the LC duration (alone) does not constrain these parameters to high accuracy.
- R_0 replaces κ as a parameter. But weak dependency also for R_0.

We know that RSGs have $R_0 \sim 500\ R_{\odot}$. If we assume $E_{51} = 1$, their typical observed diffusion duration of 120d gives from Eq. 16 a mass estimate $M \sim (120\mathrm{d}/40\mathrm{d})^{8/3} \sim 18\ M_{\odot}$.

One may also replace R_{phot} in Eq. 13 not by $R_{phot}(t) \approx$ constant $\approx v_{max} \times \frac{\Delta t_{IIP}}{2}$ but instead by the diffusion equation (Eq. 10). Then (still combining with Eq. 15) one gets

$$\boxed{\Delta t_{IIP} = 81\mathrm{d}\ E_{51}^{-1/6} M_{10}^{1/2} R_{0,500}^{1/6} \kappa_{0.2}^{1/6}} \tag{17}$$

These analytic considerations are not only useful for simple fitting procedures. *They fundamentally tell us about sensitivities and what is likely to be possible to determine by comparing detailed numeric light curve simulations to observations.* For example, it is clear that E and R_0 cannot readily be extracted from a Type IIP SN LC duration, no matter how detailed model. The weak scaling also give us a first explanation for the relative similarity of IIP light curves durations; they all have rather similar length ($\sim$120d). As different progenitors would still have R_0, E and M similar to factor few (RSGs don't vary by more than that in properties), the variety in Δt_{IIP} is, from Eq. 17 quite small.

What about trying to extract the ejecta mass from the LC duration? Here the scalings are less weak than for E and R_0 so the situation looks more encouraging. Somewhat surprisingly, only in 2003 was the first systematic attempt to do this carried out (Hamuy 2003). But something went terribly wrong - the derived masses were often much larger $(30, 40, 50..M_{\odot})$ than any reasonable RSG mass.

The most important shortcoming of the analytics derived so far is the omission of **radioactive decay**, which turns out to have a significant impact on the LC duration of Type IIP SNe, and was the reason these early attemps went astray. Remember there is a source term $s(m,t)$ in the energy equation which we have ignored so far.

To include this effect in a simplified way, make an ansatz that the extra internal energy generated by radioactivity can be approximated to be deposited at $t = t_{decay}$, and then degrades with t^{-1} just as the initial explosion deposited energy. We get one term for each step in the 2-step decay ^{56}Ni $\rightarrow^{56}$ Co $\rightarrow^{56}$ Fe:

$$E_{int}(t) = E_0 \frac{t_0}{t} + E_{\rm Ni} M_{\rm Ni} \frac{\tau_{\rm Ni}}{t} + E_{\rm Co} M_{\rm Ni} \frac{\tau_{\rm Co}}{t} \tag{18}$$

where t_0 denotes the shock breakout time $t_0 = R_0/v_{shock} \approx R_0/v_{max} \approx R_0 E^{-1/2} M^{1/2}$. $E_{\rm Ni}$ and $E_{\rm Co}$ are the total radioactive decay energies released by a solar mass of ^{56}Ni and ^{56}Co, respectively, and $\tau_{\rm Ni}$, $\tau_{\rm Co}$ are the respective decay times of 8.8d and 111d. The above can be rewritten

$$E_{int}(t) = E_0 \frac{t_0}{t} \times f \tag{19}$$

$$f = \left[1 + C M_{\rm Ni} E^{-1/2} M^{-1/2} R_0^{-1}\right] \tag{20}$$

In the derivations above, the light curve duration scales with $E_0^{1/6}$ through a $E_{int}^{1/6}$ dependency (don't confuse with overall $E^{-1/6}$ scaling where also the ejecta velocity enters). Thus, with the introduced boosting factor we expect that we get a modified light curve duration according to

$$\Delta t_{IIP}^{with-radioactivity} = \Delta t_{IIP} \times f^{1/6} \tag{21}$$

Comparison to numeric simulations show that this scaling holds quite well, and for typical ^{56}Ni masses the plateau is lengthened by ∼20% due to the impact of sustained heating by ^{56}Co. However, the value of the C coefficient, and thereby what exactly this lengthening factor is, depends on assumptions about the ^{56}Ni mixing. Goldberg 2019 find, when units of M_{10}, E_{51}, $R_{0,500}$ are used in Eq. 20, a best value $C = 87$ (so $f_{rad} = 3.61$ for $M_{Ni} = 0.03\ M_\odot$ and $M_{10} = E_{51} = R_{0,500} = 1$).

Thus, with consideration of radioactivity, an upgrade of Eq. 17 becomes (where $M_{56Ni,0.03}$ is $M_{56Ni}/0.03\ M_\odot$)

$$\boxed{\Delta t_{IIP} = 81\text{d}\ E_{51}^{-1/6} M_{10}^{1/2} R_{0,500}^{1/6} \kappa_{0.2}^{1/6} \times \left(1 + 2.6 M_{\rm 56Ni,0.03} E_{51}^{-1/2} M_{10}^{-1/2} R_{0,500}^{-1}\right)^{1/6}} \tag{22}$$

3 Light curve brightness

3.1 Explosion-deposited energy

3.1.1 Constant opacity

The brightness scale can at first instance be estimated as the internal energy at time Δt divided by the diffusion time $t_{diff} \approx \Delta t$. Using again the adiabatic

limit:

$$L \approx \frac{E/2(R(t=\Delta t)/R_0)^{-1}}{\Delta t} = \frac{E/2R_0}{v_{max}\Delta t^2} = \frac{E/2R_0}{\left(\frac{10}{3}\right)^{1/2} E^{1/2} M^{-1/2} \Delta t^2} \tag{23}$$

Insert now $\Delta t = 20\text{d}\ E_{51}^{-1/4} M_{M_\odot}^{3/4} \kappa_{0.2}^{1/2}$ from Eq. 12. Then

$$\boxed{L \approx 6 \times 10^{42} E_{51} M_{M_\odot}^{-1} R_{0,500} \kappa_{0.2}^{-1}\ \text{erg s}^{-1}} \tag{24}$$

We make the following observations

- **Brightness increases (linearly) with** E. This is not quite as simple as "put twice as much energy in and twice as much comes out". Higher E leads to a larger energy reservoar (E^1 factor), but also to higher velocities, which gives stronger adiabatic degradation to a given radius ($E^{1/4}$ factor). But this is offset by a shorter diffusion time ($E^{-1/4}$ factor), so these two effects cancel and leave only the first one.
- **Brightness increases (linearly) with** R_0. This is because larger R_0 means less adiabatic cooling can occur for a given elapsed time. Compact stars like Wolf-Rayet and bare He cores have $R_0 \sim$ few $R_\odot$. Then, without further energy input they would peak at about 10^{40} erg s^{-1} according to 24. Explosion of white dwarfs ($R_0 \sim 0.01 R_\odot$) would peak at 10^{38} erg s^{-1}.
- **Brightness decreases (linearly) with** M. Increasing M leads to lower velocities, higher densities, and more trapping of the radiation. The radiation leakage out from the SN then gets spread out over a longer diffusion time ($M^{3/4}$ factor), and also degrades more adiabatically ($M^{1/4}$ factor).
- **Brightess decreases (linearly) with** κ. Spreading the energy release over a longer diffusion time both dilutes by the time itself ($\kappa^{1/2}$ factor) and leads to more adiabatic degradation over this longer time ($\kappa^{1/2}$ factor).

3.1.2 Type IIP SNe

With the alternative derivation for Type IIP SNe, if one eliminates Δt_{IIP} instead of L from Eqs. 14 and 15, one gets

$$L \propto E^{3/4} M^{-1/4} R_0^{1/2} T_{rec}^2 \tag{25}$$

All scalings here are weaker than in Eq 24. Considering both equations, the brightness appears mainly a potential diagnostic of E, but also this dependency is sublinear.

If one instead solves for L from Eqs. 13, 15 and 10 one gets instead

$$L \propto E^{5/6} M^{-1/2} R_0^{2/3} \kappa^{-1/3} \tag{26}$$

One may stop and ponder the question, why is R_0 is parameter on par with M and E in the analytic scalings? After all, doesn't a stellar evolution model predict R_0 given M? Not quite. It would predict M and R_0 given a M_{ZAMS}. But, 1) There could be degeneracy in this even with perfectly known physics, i.e. two different M_{ZAMS} could give similar M and R_0, and 2) the generally held view is that the uncertainties in such mapping are too large to make it meaningful to rely on those predictions. For example, the envelopes of RSGs are quite poorly understood so even a link between M and R_0 is poorly constrained theoretically. Therefore, the approach of keeping both M and R_0 as free parameters remains a popular and viable approach.

To know how accurate the analytic scalings are, they have to be compared to numeric LC simulations. In the literature such work is quite recent. Goldberg 2019 take the approach to keep the scaling exponents of M, E, and R_0, drop out κ and T_{rec}, and then fit the overall scale constants governing L and Δt_{IIP}. For luminosity on day 50, they determine that a relation (keeping the analytically derived exponents):

$$L_{50} = 1.5 \times 10^{42} M_{10}^{-1/2} E_{51}^{5/6} R_{0,500}^{2/3} \text{ erg s}^{-1} \tag{27}$$

agrees with L_{50} obtained in a grid of advanced numeric models (where evolutionary progenitors were used) to an rms of 8%. By letting also the exponents float in the fitting, an alternative relation

$$L_{50} = 1.4 \times 10^{42} M_{10}^{-0.40} E_{51}^{0.74} R_{0,500}^{0.76} \text{ erg s}^{-1} \tag{28}$$

reduces the rms to 5%. Noteworthy here is how close the best-fitting exponents are to the analytically derives ones.

Goldberg 2019 combine their free-fitted formulas for L_{50} and Δt_{IIP} (large ^{56}Ni mass limit) to derive inverted expressions for M and E as function of observables plus a specified R_0. They then recover M and E with an rms of 10%. They emphasize that it is in fact not possible to derive all of the three parameters M, R_0 and E from a IIP light curve which really has only two pieces of information : brightness level and duration.

3.2 Radioactivity

Table 1 shows the peak brightness of different transients predicted by Eq. 24 and observed ones. *It is clear that, apart from Type IIP SNe, shock deposited energy diffusing out is not the correct explanation for SN brightness.* Instead, the bulk energy release by Type II-pec, Type Ibc and Type Ia SNe has its origin in radioactive powering. The most important radioisotope in SNe is ^{56}Ni, which decays to ^{56}Co on a time-scale of 8.8d, and then to ^{56}Fe on a time-scale of 111.4d. A total ^{56}Ni mass of $\sim 0.05\ M_\odot$ is produced in CCSNe and $\sim 0.5\ M_\odot$ in Type Ia SNe. The Q-value is 5.5 MeV/decay so the total decay energy is

$$E_{decay} \approx \frac{M(^{56}\text{Ni})}{56 m_p} \times 5.5 \times 10^6 \text{ eV} \approx 2 \times 10^{49} \left(\frac{M(^{56}\text{Ni})}{0.1\ M_\odot} \right) \text{ erg} \tag{29}$$

where 1 eV $= 1.6 \times 10^{-12}$ erg was used. *This is over 20 times smaller than the energy deposited in the explosion, but it is released into the SN ejecta over a long time-scale which avoids the strong adiabatic degradation of the shock-deposited energy (which is a factor* $\sim 10^4$ *for* $R_0 = 1\ R_\odot$ *and* $t = 10d$*).*

Star	SN type	R_0 ($R_\odot$)	L_{peak} (Explosive, Eq 24) (erg/s)	L_{peak} (Observed) (erg/s)
RSG	IIP	500	6×10^{41} ($M_{M_\odot} = 10$)	$3 \times 10^{40} - 3 \times 10^{42}$
BSG	II-pec	50	6×10^{40} ($M_{M_\odot} = 10$)	$\sim 1 \times 10^{42}$
WR star	Ibc	5	6×10^{39} ($M_{M_\odot} = 10$)	$\sim 1 \times 10^{42}$
WD	Ia	0.01	1×10^{38} ($M_{M_\odot} = 1$)	$\sim 1 \times 10^{43}$

Table 1: Peak luminosities of different SN classes predicted by shock leakage models compared to observed ones.

One can estimate that to within factor 2 or so, radioactive powered LCs has a peak luminosity that is close to the radioactive decay power at that time. This is called "Arnett's law"

$$\boxed{L_{peak} \approx S(t_{peak})} \tag{30}$$

where $S(t)$ denotes the total energy injection rate ($S(t) = \int_{m=0}^{M} s(m,t)dm$). This is useful to estimate the ^{56}Ni mass in such SNe. For example, ^{56}Co decay obeys roughly

$$S(t) = 1.4 \times 10^{42} \left(\frac{M(^{56}\mathrm{Ni})}{0.1\ M_\odot} \right) \exp\left(-t/111\ \mathrm{d}\right)\ \mathrm{erg\ s^{-1}} \tag{31}$$

The peak time can be estimated by equating $t_{diff} = t$, as before.

3.3 Surface temperature and spectral shape

Define the photosphere R_{phot} as the radius from which photons can escape freely (τ =1, or sometimes $\tau = 2/3$). Assume for now this is wavelength independent. Assuming blackbody emission, we have

$$L(t) = 4\pi R_{phot}(t)^2 \sigma T_{phot}(t)^4 \tag{32}$$

With homology $R_{phot}(t) = V_{phot}(t)t$ so

$$T_{phot}(t) = \left(\frac{L(t)}{4\pi\sigma V_{phot}(t)^2} \right)^{1/4} t^{-1/2} \tag{33}$$

For an order of magnitude estimate, take typical $L_{peak} = 10^{42}$ erg s^{-1}, $t_{peak} =$ 30d and $V_{phot} = 5000$ km s^{-1}, $\rightarrow T_{phot} \approx 5000$ K. Thus, SNe peak at "optical temperatures".

For the radioactivity peak:

- During pre-peak: L is increasing (and V_{phot} is always decreasing as more and more layers become transparent) so T_{phot} either declines *slower* than $t^{-1/2}$ or increases.
- Around peak: L is roughly constant (the peak defines its zero derivative), V_{phot} is slowly decreasing, so T_{phot} follows $t^{-1/2}$ or somewhat slower. Having reached peak L and the SED peaking at longer wavelengths with time means that *longer-wavelength bands peak later*.
- During post-peak: L is now decreasing so rapidly that the evolution is typically faster than $t^{-1/2}$.

Figure 1 shows an observed evolution in these three phases. Typically, observations of L and T_{phot} are used to determine the $R_{phot}(t)$ evolution, which constrains models. At about twice the peak time, the diffusion is over and the SN enters the nebular phase. The assumption of a photosphere emitting a blackbody then breaks down.

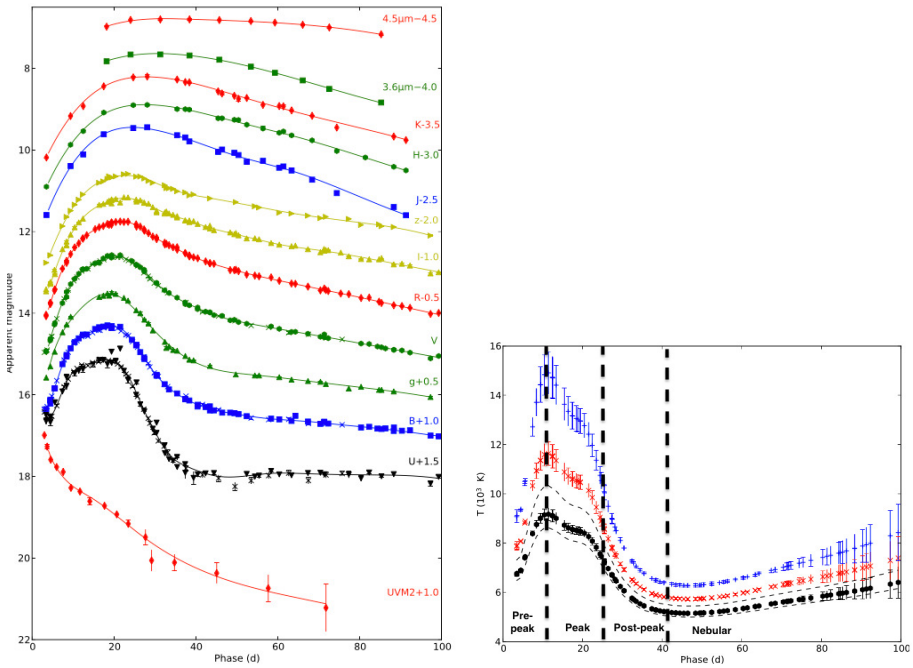

Figure 1: Evolution of the light curves in different photometric bands (left) for a radioactivity-powered Type IIb SN and (right) the T_{phot} evolution (black symbols, ignore other plotted quantities). From Ergon et al. 2014.

From an observed radioactive powered light curve, can we determine M, E?

Our observable is basically the light curve duration, which should be similar to the diffusion time, then depending on $E^{-1/4}M^{3/4}\kappa^{1/2}$. We have three variables but only one observable so we have to come up with two more relations. The first is easy - pick an opacity! The second is to measure some velocity and use this to link M and E - more on this in the spectral part of the course.

4 The diffusion term

What about the energy transport term $\partial l(m,t)/\partial m$ in the 1st law of TD?

$$\frac{\delta u(m,t)}{\delta t} = s(m,t) - \frac{\partial l(m,t)}{\partial m} - p(m,t)\frac{\partial 1/\rho(m,t)}{\partial t} \tag{34}$$

In the diffusion limit (see stellar structure equations in Part A)

$$l = \left(4\pi r^2\right)^2 \frac{c}{3\kappa}\frac{daT^4}{dm} = \frac{16\pi^2 c}{3\kappa} r^4 \frac{daT^4}{dm} \tag{35}$$

Then

$$\frac{\partial l}{\partial m} = \frac{16\pi^2 c}{3\kappa}\frac{\partial}{\partial m}\left(r^4\frac{daT^4}{dm}\right) \tag{36}$$

In general, to include this we have to solve the PDE numerically. Such solutions show the term becomes important after about 3-4 weeks for Type II SNe. The term can also be considered in certain semi-analytic frameworks.

5 The post-diffusion phase : the radioactive tail phase

When the diffusion phase is over (after few months) we enter the *tail phase*. Here, the nebula is now so expanded and optically thin than any energy deposited is quickly reradiated so:

$$L(t) = S(t) \tag{37}$$

The gamma rays from radioactive decay are not trapped forever : in fact for most SNe already at the beginning of the tail phase they start to leak out. Thus, for Type II-pec, Ibc, and Ia SNe, there is another constraint available here from the degree of trapping observed - this depends on the ejecta optical depth to gamma rays $\tau_\gamma \propto M v_{max}^{-2} t^{-2} \propto M^2 E^{-1} t^{-2}$.

For Type IIP SNe, observations in the tail phase are needed to determine the ^{56}Ni mass - this is not making itself straightforwardly known during the diffusion phase as it does for the other SN classes (see Arnett's law).

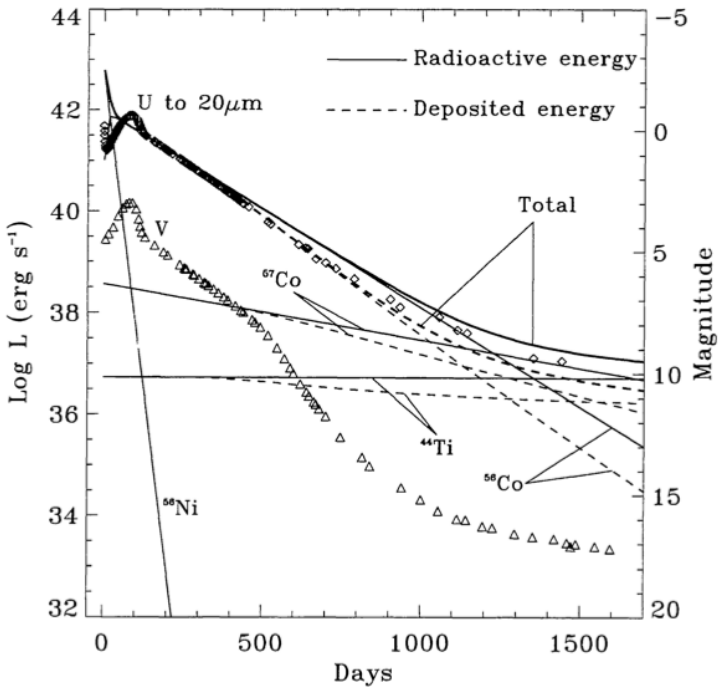

Figure 2: The bolometric light curve of SN 1987A from explosion to 1500 days later. The progenitor was compact (50 $R_\odot$) so the shock deposited energy was rapidly adiabatically degraded and the light curve was initially fast declining. Decay by ^{56}Ni/^{56}Co then gave a radioactivity powered diffusion with peak at around 80d. The tail phase started at around 150d when output closely followed the radioactive input. Gamma rays started leaking out at around 400d. After 1000d, ^{57}Co and ^{44}Ti started affecting the light curve. From McCray 1993.

Going to times beyond ∼2y after explosion, other radioisotopes than ^{56}Co may start to affect the light curve (e.g. ^{57}Co, ^{44}Ti), as can other source of energy such as circumstellar interaction or energy input from the central neutron star. Most SNe are however difficult to observer so late, so the very late phases are little explored. An exception is the nearby SN 1987A (Fig. 2).

6 The opacity of supernovae

Opacity is a key quantity that directly affects the degree of trapping of radiation and from that both light curve durations and brightness levels. It is therefore important to understand its behavour and typical values.

The interaction of photons and matter is dominated by photon-electron interactions. The electron can be free or bound in an atom, molecule or dust grain. We will consider four main processes: electron scattering, free-free absorption, photoionization and line absorption.

6.1 Electron scattering

In the frame of the electron, for $E_{photon} \ll m_e c^2(511 \text{ keV})$, to good approximation photons scatter, i.e. change direction but not energy. This is called Thomson scattering. This is for most SNe an important source of interaction. The cross section is wavelength-independent ("gray") : $\sigma_T = 6.7 \times 10^{-25}$ cm^2. Then, letting n_e denote the number density of free electrons and $n_{nucleons}$ the number of protons and neutrons, free and bound, per unit volume:

$$\kappa^{es} = \frac{n_e \sigma_T}{\rho} = \frac{n_{nucleons} Y_e x_e}{n_{nucleons} m_p} = 0.4 Y_e x_e \text{ cm}^2\text{g}^{-1} \tag{38}$$

where $Y_e = n_e/(n_{nucleons}) = (1-\eta)/2$ is the electron fraction, $x_e = n_e/n_{atoms/ions}$ is the ionization degree (0-1). Examples:

- Pure H, fully ionized : $Y_e = 1$, $x_e = 1$, $\rightarrow \kappa^{es} = 0.4$ cm^{2}g^{-1}.
- Pure He, singly ionized: $Y_e = 0.5$, $x_e = 0.5$, $\rightarrow \kappa^{es} = 0.1$ cm^{2}g^{-1}.

All elements except H have $Y_e \approx 0.5$. If half ionized, $\kappa^{es} = 0.1$ cm^2 g^{-1}. This is an often used value of κ^{es} when little else known.

At $E_\gamma \gtrsim m_e c^2$, the recoil energy of the electron becomes a significant fraction of the energy budget: the scattering becomes incoherent as the photon loses a significant fraction of its energy to this recoil motion. In this limit (called Compton scattering), the cross section is smaller, declining with energy. At $E_{photon} = 1$ MeV is is about 1/3 of σ_T.

How long is a SN of mass M and kinetic energy E optically thick to electron scattering?

$$\tau_{es} = \kappa^{es} \rho R = \kappa^{es} \frac{M}{4\pi/3 R^2} = \kappa^{es} \frac{M}{4\pi/3 v_{max}^2 t^2} = \kappa^{es} \frac{M^2}{40\pi/9 E t^2} \tag{39}$$

Putting $\tau_{es} = 1$ we get

$$\boxed{t^{es}_{thick} = 120\text{d} \ \left(\kappa^{es}_{0.4}\right)^{1/2} M_{M_\odot} E_{51}^{-1/2}} \tag{40}$$

But Type IIP SNe have $M_{M_\odot} \approx 10$ and then we get $t_{thick} = 1600$d. We know that they become optically thin to electron scattering much earlier, around 100-200d when they enter the tail phase. The reason for the discrepancy is that they continously recombine, so $\kappa^{es}_{0.4} \sim 1$ is not accurate. By 200d, $x_e \sim 0.01$, which brings $\kappa_{0.4}$ down to $\sim$0.01, and t^{es}_{thick} down to 195d.

What about Type Ia SNe? They have $\sim 1\ M_\odot$ ejecta of mostly iron. Spectra tell us ejecta are roughly doubly ionized, so $x_e \sim 2/26 = 0.08$, so $\kappa^{es} = 0.016$, and $t^{es}_{thick} \approx 25$d. Similar parameters hold for Type Ibc SNe, so we conclude these remain optically thick with respect to electron scattering for a few weeks.

6.2 Free-free absorption

A photon can be absorbed by an electron in the presence of a third positively charged body such as a proton or a He+ ion. Averaged of a thermal distribution of electrons:

$$\boxed{\kappa^{ff}_\lambda = 0.8 T_4^{-1/2} \lambda^3_{\mu m} \left(1 - e^{-hc/\lambda kT}\right) \left(\frac{n_e}{10^{13}\ \mathrm{cm}^{-3}}\right) Z^2 A^{-1}}\ \mathrm{cm}^2\mathrm{g}^{-1} \qquad (41)$$

Here $T_4 = T/10^4$K, Z is the charge of the ion and A its atomic number. Two important properties are:

- For a blackbody field the bulk of radiation has $hc/\lambda \geq kT$, so the $1 - \exp(-hc/\lambda kT)$ term is close to unity.
- While κ^{es} is independent of n_e, κ^{ff}_λ is proportional to it (due to its 3-body nature). The opacity then evolves more rapidly in time, declining (because n_e has a rapid decline as approximatelty $\propto t^{-3}$) unless T would decline more rapidly than t^{-6} to offset.[1]

In practice, free-free absorption plays only a secondary role for energy transport for the following reason; the density needs to be high for κ^{ff} to be large, but at high density, i.e. early on in the SN evolution, the temperature is also high and then $\lambda^3_{\mu m}$ for the radiation field is small. Thus, in no regime are both of these factors favorable at the same time.

Free-free opacity plays, however, an important role for what light emerges in the infrared. For example, at $\lambda \gtrsim 10\ \mu$m the SN can remain optically thick for many months.

6.3 Photoionization

A photon can eject a bound electron in a photoionization, if $E_{photon} > E_{binding}$. This is also called bound-free absorption. For hydrogen and hydrogenic ions

$$\sigma^{pi}_\lambda \approx 10^{-17} \left(\frac{\lambda}{\lambda_0}\right)^3\ \mathrm{cm}^2 \qquad (42)$$

[1] We know however, e.g. from the adiabatic limit solution ($T \propto t^{-1}$) that this is not the case.

where λ_0 is the ionization threshold ($= hc/E_{binding}$), which is 912 Å for the ground state of hydrogen. Then, for H at $\lambda < \lambda_0$ (the opacity is zero for $\lambda > \lambda_0$)

$$\kappa_\lambda^{pi} = \frac{\sigma_\lambda^{pi}(1-x_e)}{m_p} = 6 \times 10^6 (1-x_e) \left(\frac{\lambda}{\lambda_0}\right)^3 \ \mathrm{cm^2 g^{-1}} \tag{43}$$

Clearly, as long as even a minor amount of H is neutral ($1 - x_e \gtrsim 10^{-7}$), κ_λ^{pi} is much larger than both κ^{es} and κ_λ^{ff} at wavelengths close to threshhold. Some other element thresholds:

Element	λ_0
He I	504 Å
O I	912 Å
O II	353 Å
Fe I	1568 Å
Fe II	766 Å
Fe III	404 Å

Table 2: Photoionization ground state threshholds for some common atoms and ions.

If the radiation field peaks in the UV ($\lesssim$ 1500 Å) where many photons are at wavelengths below the threshholds, photoionization can be expected to be important. From Wien's displacement law, $\lambda_{peak} = 0.29/T$ cm, giving $T \gtrsim 20,000$ K for this condition. However, at higher T the atoms tend to be in higher ionization states for which the threshhold energies are larger.

At later times the gas becomes more neutral ($1 - x_e \to 1$) and one might expect κ^{pi} to gain in importance. However, then $T \ll 20,000$ K and few photons have enough energy. As for free-free absorption, two conditions are required which are not easily met at the same time in the SNe and therefore photoionization plays a limited role for the energy transport. While free-free absorption still played a role for the emergent IR light, photoionization plays a corresponding role for emergent UV light.

Excited states. The thresholds λ_0 move to longer wavelengths for photoionization from excited states, e.g. n=2 in H I has a threshold at 3646 Å. A significant fraction of photons have such energies for $T \gtrsim 5000$ K. However, the number of atoms in these excited states is typically much smaller than in the ground state.

Figure 3 shows a figure illustrating optical depths arising from the opacities discussed so far in a toy model for a Type II SN at 150d.

6.4 Line absorption

A photon can be absorbed and cause a photoexcitation of a bound electron from a lower state l to an upper state u. This is also called a bound-bound transition.

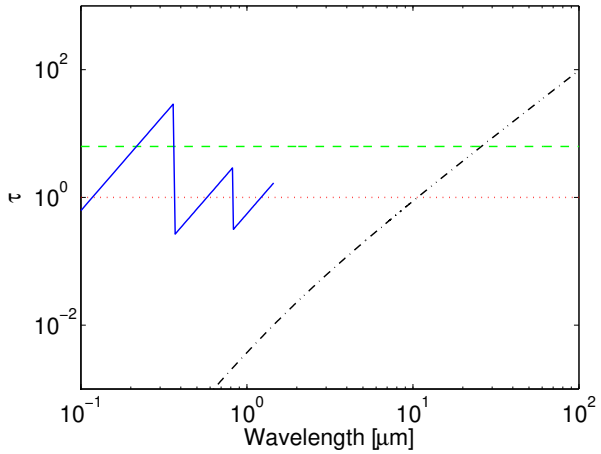

Figure 3: Optical depths in continuum processes in a model for a Type II SN at 150d. Blue: photoionization, green: electon scattering, black: free-free. From Jerkstrand 2011.

The cross section can be written

$$\sigma_\lambda^{bb} = \Phi_0 \phi(\lambda - \lambda_0) \tag{44}$$

where ϕ is the line profile (unit cm^{-1}), which is normalized so $\int_{-\infty}^{+\infty} \phi d\lambda = 1$. The strength of the line is given by the parameter

$$\Phi_0 = \frac{h\lambda_0}{4\pi} B \tag{45}$$

where B is the Einstein absorption coefficient (unit cm^2 ster erg^{-1} s^{-1}), which can be of order 10^{10} for strong lines, giving $\Phi_0 \sim 10^{-22}$ cm^3 in the optical. Thermal broadening is of order $v_{th} = \sqrt{kT/m_p} \sim 1$ km s^{-1}, or $\Delta\lambda_{th} = \lambda_0 v_{th}/c \sim 0.01$ Å(taking $\lambda_0 = 3000$ Å), so $\sigma^{bb} \sim 10^{-12}$ cm^2 for a strong line if we take $\phi \sim 1/\Delta\lambda$. Then, for a box-like profile

$$\kappa_{\lambda 0}^{bb} = \frac{\sigma^{bb}}{m_p} = \frac{h\lambda_0}{4\pi} B \frac{1}{\Delta\lambda_{th} m_p} \sim 10^{12} \text{ cm}^2\text{g}^{-1} \tag{46}$$

A line can provide huge opacity over its profile, 10^{12} times electron scattering, but if the photon field covers say 10^4 Å, only a fraction $0.01/10^4 = 10^{-6}$ would have the precise energy needed to interact with the line. It is clear that to understand line opacity, we must obtain information on the total number of lines with significant opacity - if there are only a few they will not be able to play a role, but if there are thousands or millions of them they are able to provide opacity over most of the wavelengths of the radiation field.

The excited atom typically relaxes back by spontaneous emission (rate A s^{-1}, where A is the Einstein emission coefficient), either in the same transition ("resonance scattering") or in a set of branching ones ("fluorescence"). It can also be collisionally deexcited by a free electron ("thermalization"), but the chance of this is typically quite small.

6.4.1 Expansion effects

There are three frames of relevance for understanding the link between the SN flow and and the effect of Doppler frequency shifts introduced by this motion : the SN **centre-of-mass frame** , the **comoving frame**, and the **interaction frame**.

- The centre-of-mass frame is the frame in which the net velocity vector disappears. It equals the observer frame apart from any bulk motion of the SN towards or away from us.
- The comoving frame is the frame (varying from point to point) where the net velocity of particles is zero : thus the frame is moving along with the bulk velocity of the gas at the given point.
- The interaction frame is the frame in which the absorbing/scattering particle is at rest : it differs from the comoving frame because of the particular thermal motion of the particle.

Material from an explosion, like the galaxies in the Universe (from Big Bang) or the layers in a supernova, move at different velocities described by homology $v \propto r$. One may show that in such homologous flows, each point sees the other points moving radially away from it with velocity proportional to the distance (think of Hubble's law for galaxies). If a photon is emitted at a comoving wavelength λ_1 at point 1, when it arrives at point 2, moving away from point 1 with relative velocity Δv, it will have a redshifted comoving wavelength

$$\lambda_2 = \lambda_1 \left(1 + \frac{\Delta v}{c}\right) \tag{47}$$

Thus, as a photon travels from point to point, it is continously redshifted in each local, comoving frame.

Consider what this means for transfer through lines. If emitted in a frame with comoving wavelength λ_{start}, the photon will come into resonance with a line at $\lambda_0 (> \lambda_{start})$ only after travelling a distance corresponding to velocity difference $\Delta v = c \times (\lambda_0/\lambda_{start} - 1)$. Giving the line profile a finite width $\Delta\lambda$ (given by thermal motions), the interaction region is a small length interval corresponding to where the comoving wavelength is in the range $\lambda_0 - \Delta\lambda/2$ to $\lambda_0 + \Delta\lambda/2$. This length is called the Sobolev length.

In supernovae $v/c \sim 0.01 - 0.1$. This is much larger than the thermal line widths: $v_{th}/c \sim 10^{-5}$. This means that

A The Sobolev length is much smaller than the radial scale of the SN and a given photon interacts in a small local region with any given line.

B A photon can sequentially come into resonance with many lines, at sequential points along its path. If there is a distance v_{edge} to the edge of the nebula (as perceived from the emitting frame), the photon will be exposed to absorption by all lines with rest wavelengths lying in the range from λ_{start} to $\lambda_{start} \times (1 + v_{edge}/c)$.

Property (A) means a *simplification* of the line transfer process as each interaction can treated as a local event and whether absorption happens or not depends just on local gas conditions, and there is no dependency on detailed line profile shapes. Property (B) means a *complication* compared to static nebulae, where any given photon only interactions with a single line, as we here we have to consider multiple ones.

A) Local line interaction (The "Sobolev limit"). The photon will 'traverse' the line profile over a length $L_{Sob} = v_{th}/(dv/dr)$, where dv/dr is the velocity gradient. As $v = r/t$ in homology, $dv/dr = 1/t$ and $L_{Sob} = v_{th}t$. As $v_{th} \ll v$ this region is small compared to the size of the SN. For a top-hat line profile ($\phi = 1/\Delta\lambda_{th}$):

$$\boxed{\tau_{Sob} = \sigma n_l L_{Sob} = \frac{h\lambda_0}{4\pi} B \frac{1}{\Delta\lambda_{th}} \times n_l \times \frac{\Delta\lambda_{th}}{\lambda_0} ct = \frac{hc}{4\pi} B n_l t} \tag{48}$$

One can show that this holds for *any* line profile. The optical depth depends only on the local number density (n_l) at the point of resonance. Ignoring changes in ionization/excitation, $n_l \propto t^{-3}$, so $\boxed{\tau_{Sob} \propto t^{-2}}$.

B) Expansion opacity. If there is a typical velocity separation Δv_{sep} between optically thick lines around wavelength λ, the mean-free path is $\lambda_{mfp} = \Delta v_{sep} t$ (note we use now λ for both mean-free-path and wavelength, the former has a $_{mfp}$ subscript). Write $\Delta v_{sep} = c\Delta\lambda_{sep}/\lambda$. Then, since $\kappa = 1/(\lambda_{mfp}\rho)$,

$$\boxed{\kappa_\lambda^{line,exp} \approx \frac{\lambda}{ct\rho\Delta\lambda_{sep}}} \tag{49}$$

A more refined formula can be obtained from knowing the probability that line i interacts is $1 - \exp\left(-\tau_{Sob}^i\right)$. Then refine the formula as

$$\boxed{\kappa_\lambda^{line,exp} \approx \frac{1}{ct\rho} \frac{1}{N} \sum_{i=1}^{N} \frac{\lambda_i}{\Delta\lambda_i} \left(1 - e^{-\tau_{Sob}^i}\right)} \tag{50}$$

where the set of N lines have to be chosen over some wavelength range centred on λ.

This is called an expansion opacity. Figures 4 shows an illustration. Note that this is not an exact local opacity like the other ones - this is because

line interaction is not a continuous process but occurs at discrete points in the Sobolev limit. As opacity can only be defined as some integral/summation over lines, there is always some degree of arbitrariness how this is done - N is basically a free parameter in Eq. 50. Line opacity is together with Thomson opacity typically the most important in SNe.

6.5 What happens to the energy?

Consider now Table 2, summarizing what happens to the radiative energy following an absorption. Three things can happen : 1) reemission of the photon (scattering or fluorescence), 2) thermalization (photon energy goes to kinetic energy of particles), or 3) raising the potential energy of gas particles.

In many situations Thomson scattering and line absorption are the dominant opacities. But neither of these couple strongly to the thermal energy of the gas - the photon tends to get reemitted again. Even if they happen less often, free-free and bound-free absorption play an important role in providing this coupling, which resets the distribution and brings conditions close to "local equilibrium" where the radiation field obtains a temperature linked to the local gas temperature.

Process	Scattering/Fluorescence	Thermalization	Potential energy
Thomson	100%	0%	0%
Free-free	0%	100%	0%
Bound-free	0%	Part	Part
Line	Mostly	Minor	0%

Table 3: A summary of the fate of the radiative energy following an absorption.

Finally, for line absorption fluorescence is often a more frequent deexcitation process that scattering back into the same transition (Fig. 5). Complex fluorescence means the emergent spectra of SNe are, in detail, complex to model. In particular at late times several years after explosion, models have shown that the whole optical spectrum of SN can come from fluorescence of UV emission.

7 Line formation in early ("photospheric") phases

Because $v = rt$, all points on a sheet perpendicular to the line of sight (LOS) have the same LOS velocity and give the same Doppler shift relative to the observer (Fig. 6). If the sheet is emitting in a line with rest wavelength λ_0, the observer will see emission at wavelength $\lambda_0 \times (1 + v_{los}/c)$, where positive projected velocity v_{los} is defined to be away from the observer. If the line absorbs, the sheet is capable of blocking photons at that wavelength, in the observer frame, travelling from the region it covers from the observer.

The scattering atmosphere (also called the Schuster-Schwarzschild model) is a simplified model framework where blackbody radiation is emitted from an inner

boundary - the photosphere - and then scatters (by electron scattering and line scattering) in the outer layers. It is a simplified concept because in a real supernova

- The location of the photosphere (formally defined as where optical depth integrating from outside in is $\tau_\nu = 2/3$) varies with frequency.
- Even for a fixed frequency, the photosphere does not sharply divide into a scattering only region on the outside and a thermalization only region on the inside.

In fact, advanced radiative transfer models for SN spectra do not rely on the scattering atmosphere ansatz but model also the transition region and the deeper layers. Nevertheless, it is a framework that allows a good understanding of the basic processes forming the spectrum, and rough spectral models to be developed that by comparison with observations allow reasonably accurate estimates of the density profile and composition of the scattering layer. It is the foundation for the open-source supernova spectral modelling codes SYNOW/SYN++ (Thomas 2011) and TARDIS (Kerzendorf & Sim 2014).

Consider a scattering atmosphere where line absorption is treated in the Sobolev limit. We will study what line profile arises from a single optically thick line ($\tau_{Sob} \gg 1$), with the two parameters $h = v_{phot}/v_{max}$, where v_{max} denotes the maximum velocity at which the line is optically thick, and ϵ, the "destruction probability" (probability $1 - \epsilon$ for scattering).

Consider Fig 7. We delineate two cases.

- **Case I**. $h < 1/\sqrt{2} = 0.71$. The photosphere is fully blocked by certain sheets (in B region) $\rightarrow$ complete absorption at the Doppler velocity of those sheets.
- **Case II**. $h > 1/\sqrt{2}$. The photosphere is never fully blocked blocked by a sheet $\rightarrow$ only partial absorption.

The ABC regions behave as following:

- **Region A**: The whole resonance sheet covers (part of) the photosphere. The area of the sheet grows going inwards (towards the rest wavelength), giving a deeper absorption as a larger fraction of the photosphere gets blocked.
- **Region B-Case I**: (Part of) the resonance sheet covers the whole photosphere. Complete absorption is produced throughout B.
- **Region B-Case II**: The (whole) resonance sheet covers part of the photosphere. The sheet area is constant, giving a flat bottom in the absorption

profile but at non-zero flux. The absorption depth increases with decreasing h.

- **Region C**. Part of the sheet covers part if the photosphere. A declining fraction of the photosphere is blocked moving towards the centre, giving declining degree of absorption moving towards the rest wavelength.

The bottom panels in Fig. 7 show the resulting line profiles. We see that

- **Destructive line** ($\epsilon = \mathbf{1}$). Absorption starts at $-v_{max}$ and reaches the minimum at $-v_{phot}$. It has a flat minumum that is either at flux zero, for Case I, or flux $\sqrt{1-h^2}/h^2$, for Case II. The degree of absorption then gradually declines towards the rest rest wavelength in region C.

- **Scattering line** ($\epsilon = \mathbf{0}$). Absorption is the same but now reemission adds the green flux distribution. The location of the minimum does not change. For redshifted photons from the receding side of the SN, some scattered photons are blocked by the photosphere, so the maximum possible redshift is $\lambda_0 \times \left(1 + v_{max} \times \sqrt{1-h^2}/c\right)$. *The peak is at zero shift which means the line can be readily identified.*

An important point is that absorption of photons can only remove flux on the blueshifted side of the line profile : all layers that have some blockage of the photophere are necessarily on the side towards the observer and thus have blueshifted resonance frequencies. On the other hand, reemission of absorbed photons can add flux both at blueshifted and redshifted wavelengths: scattering in sheets moving away from the observer give a redshifted emission and this emission reaches the observer unless the region is blocked by the photosphere.

Observing such lines, it appears one could determine both v_{max} ***and*** v_{phot} ***in this framework :*** v_{max} ***from the maximum blueshift absorption, and*** v_{phot} ***from either the maximum redshift emission or the AB minimum (Case I) or BC minimum (Case II). In addition, once*** v_{max} ***and*** v_{phot} ***are known,*** ϵ ***can be determined from the flux peak value at*** λ_0***.***

Knowing v_{max} one may be able to determine the density of the element at that velocity by equating the line optical depth to unity there. One should note, however, than in more realistic models the interpretation of line profiles can be more complex (see e.g. Fig 6 in Sim 2017). The line optical depth is a function of velocity and does not give a sharp boundary as here. Also, there may be emission in the line, in the atmosphere, by additional processes than resonance scattering

These kind of line profiles are called "**P-Cygni**" after their initial observations in the LBV star "P-Cygni" which has an atmosphere of rapidly outflowing gas producing lines like these.

Figure 9 shows an example of observed P-Cygni lines (from He I) in a Type IIb SNe. In the first spectra the lines are not present so apparently He I was not present in sufficient amount in the atmospheric layers then (perhaps ionized to He II, or perhaps the lower levels in He I were not excited enough). But from 10-15d the lines start to emerge. The peaks are close to the rest wavelengths, as predicted. One can quite clearly read out a maximum absorption blueshift of $v_{max} \approx 11,000$ km s^{-1}. Determining a maximum redshift emission is more difficult. The location of the minimum varies between the three lines, and with epoch. By comparing to Fig 7, can one estimate h?

7.1 Line broadening

We have so far assumed that scattering has been fully coherent in the comoving frame, so the photons just change direction but not frequency. While this is an accurate description in the interaction frame (for the type of interactions currently being considered), the interacting particle has a thermal velocity in the comoving frame. This thermal velocity is $v_{therm} \approx \sqrt{\frac{3kT}{m}}$ (from $3/2kT = 1/2mv^2$), where m is the mass of the particle. For an atom this is $v_{therm}^{atom} = 11$ km s^{-1} $(T/5000$ K$)^{1/2}$ $A^{-1/2}$, where A is the atomic number. This is negligible compared to the Doppler broadening occurring due to the SN expansions which is typically several thousand kilometers per second.

For an electron, however, it is $v_{therm}^{e-} = 480$ km s^{-1} $(T/5000$ K$)^{1/2}$. Thus electron scattering, especially repeated ones, is capable of broadening (emission) lines with $\gtrsim 10^3$ km s^{-1}. This is still quite a minor effect in SNe emitting lines from regions moving with several thousand kilometers per second. But some SNe, in particular Type IIn, emit lines also from slower-moving material, ~ 100 km s^{-1}. If these layers are hot, the line profiles may become determined by thermal broadening rather than expansion broadening.

8 Line formation in late ("nebular") phases

At later times ($\gtrsim 50 - 150$d), the photosphere disappears and we enter the nebular phase. Now, the spectrum consists of emission lines. As powering comes from radioactivity, emission comes mainly from the inner regions where ^{56}Ni resides. Figure 10 shows an example of an observed nebular spectrum illustrating the quite different nature to photospheric spectra.

8.1 Line profiles

Let us consider line profiles of emission lines arising for a few simple cases of geometry. Figure 11 shows line profiles in six cases, of which we comment on three:

- **Uniform sphere (upper left)**. Letting v_p denote the component of v_{max} perpendicular to the line-of-sight, each sheet contributes flux at wavelength $\lambda_0 v_{los}/c$ in proportion to its area which grows as $\pi\left(v_p t\right)^2 = \pi t^2\left(v_{max}^2 - v_{los}^2\right) = \pi t^2 v_{max}^2\left(1-(v_{los}/v_{max})^2\right)$. The line profile is therefore a parabola.
- **Thin shell (upper middle)**. A slice of a shell can be shown to give a constant area, so the line profile becomes a flat top.
- **Gaussian (bottom left)**. One can show that also the line profile becomes a Gaussian.

For further details of the derivations see Jerkstrand 2017, Handbook of SNe.

8.2 Luminosity

The emissivity in a line is

$$j = \frac{1}{4\pi} n_u h\nu A \beta_{Sob} \ \ \text{erg s}^{-1}\text{cm}^{-3} \tag{51}$$

where n_u is the number density of the upper level of the line, A is the Einstein A-coefficient (rate of deexcitation, dont confuse with atomic number) and $\beta_{Sob} = (1-e^{-\tau_{Sob}})/\tau_{Sob}$ is the Sobolev escape probability : the chance that an emitted photon will escape the local line resonance region rather than be reabsorbed. Consider two limits

- **Optically thin line ($\beta_{Sob} \to 1$)**. The total volume-integrated luminosity is then $L = 4\pi j \times V = N_u h\nu A = \frac{M_{ion}}{\mu_{ion}} \times f(T, n_e) h\nu A$, where the function $f(T, n_e)$ determines what fraction of the ions of this type are in state u. If this can be estimated, one may then be able to determine the mass of the ion.
- **Optically thick line($\beta_{Sob} \to 1/\tau_{Sob}$)**. Then total luminosity is now $L = V \times \frac{n_u h\nu A}{hcBn_l t}$. Because B can be related to A, this can be written $L = V \times t^{-1} \times g(T, n_e)$ where the function g determines the ratio of populations in levels u and l. Thus, if this can be estimated one can determine the volume of the emitting region.

To get either a mass or volume then, we need to know what fraction of atoms for that ion is in the upper state (optically thin case), or what the ratio of upper and lower state populations (optically thick case) are.

At high electron density, collisions dominate population and depopulation of states, and then the f and g functions depend only on temperature ("Local Thermodynamic Equilibrium (LTE)" limit). Thus, in this limit only T needs to be estimated. However, one should be careful: the f and g factors have exponential dependencies on temperature. Thus, if $\Delta E \gg kT$, where ΔE is the

excitation energy of the upper level E_u for optically thin lines and $E_u - E_l$ for optically thick ones, even small errors in the T estimate can give very different factors. The result will only be meaningful if $\Delta E \lesssim$ few $\times\, kT$.

How can T be estimated? One way is from line ratios from levels with different excitation energies. For example, [O I] 6300, 6364 and [O I] 5577 come from levels 4 and 5 in O I, respectively. Level 4 has an excitation energy of 2.0 eV and level 5 4.2 eV, so a difference of 2.2 eV. If both lines are in LTE and optically thin, their luminosity ratio is

$$\frac{L_{5577}}{L_{6300,6364}} = \frac{n_5 A_{5577}}{n_4 A_{6300,6364}} = \frac{5}{1} \times \exp\left(\frac{-2.2 \text{ eV}}{kT}\right) \times 180 \tag{52}$$

where the 5/1 is the ratio of statistical weights and 180 is the ratio of A-values. Thus, an observed line ratio can give a T estimate.

At lower densities radiative deexcitations tend to dominate collisional ones and then LTE does not hold. Then, balancing collisional excitation from the ground state (where most atoms reside) with radiative decay gives

$$C(T) n_{ground} n_e = n_u A \beta_{Sob} \tag{53}$$

where $C(T)$ is the collisional excitation rate (cm^3 s^{-1}). Thus, to know n_u here one needs to have an estimate for both T and n_e. n_{ground} can be approximated with the total atom number density.

8.3 What sets the physical conditions (T, n_e)?

The flow of energy in the SN in the nebular phase is as follows. Radioactivity deposits a certain amount of energy per unit volume and time in the form of gamma-ray Compton scattering on free and bound electrons. This creates a population of MeV Compton electrons, also called "non-thermal electrons" - that transfer their energy to the gas by ionizing, exciting and heating it as they bounce around. The ionized, excited and heated gas then emits radiation by recombination and line emission. Free-free emission is neglegible. One can show that conditions close to thermal balance prevail so the SN quickly reradiates what was deposited, therefore $L = S(t)$.

The dominant radiation channels are typically low-lying, forbidden line transitions in abundant atoms that easily become excited by thermal electron collisions - this is how the gas cools, and typically of the three deposition channels of the Compton electrons (ionization,excitation,heating), heating is the dominant one so cooling by thermal electron collisions is the dominant reemission process. The gas is typically weakly ionized so mostly neutral and singly ionized atoms are present and produce the emission (also doubly ionized in Type Ia SNe).

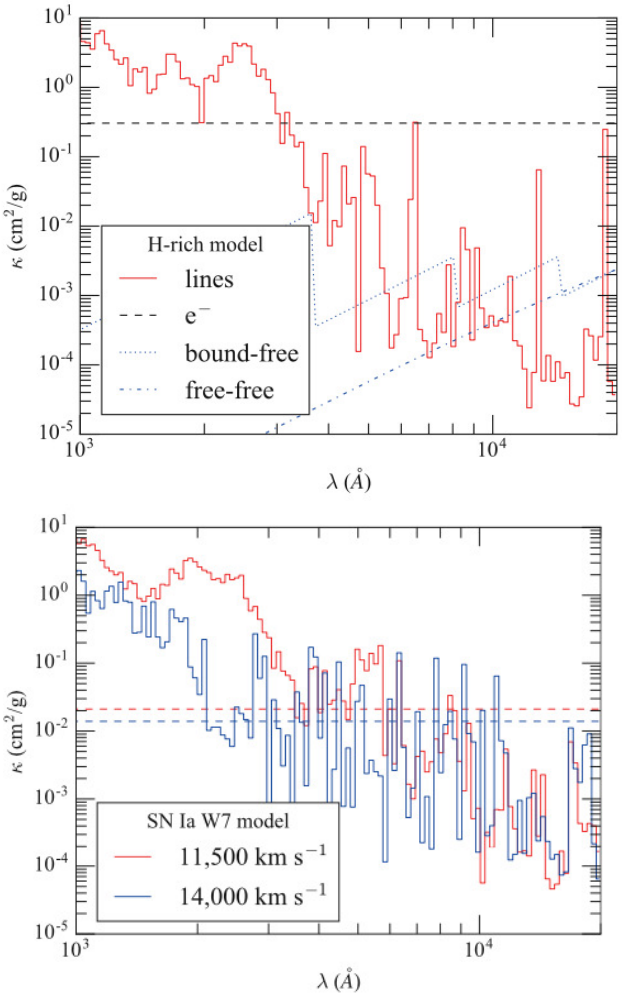

Figure 4: *Top*: Opacities in a Type IIP SN layer at 11,000 km/s at $t = 15$d. *Bottom*: Thomson opacity and line opacity in two layers in a Type Ia SN around maximum light. From Sim 2017.

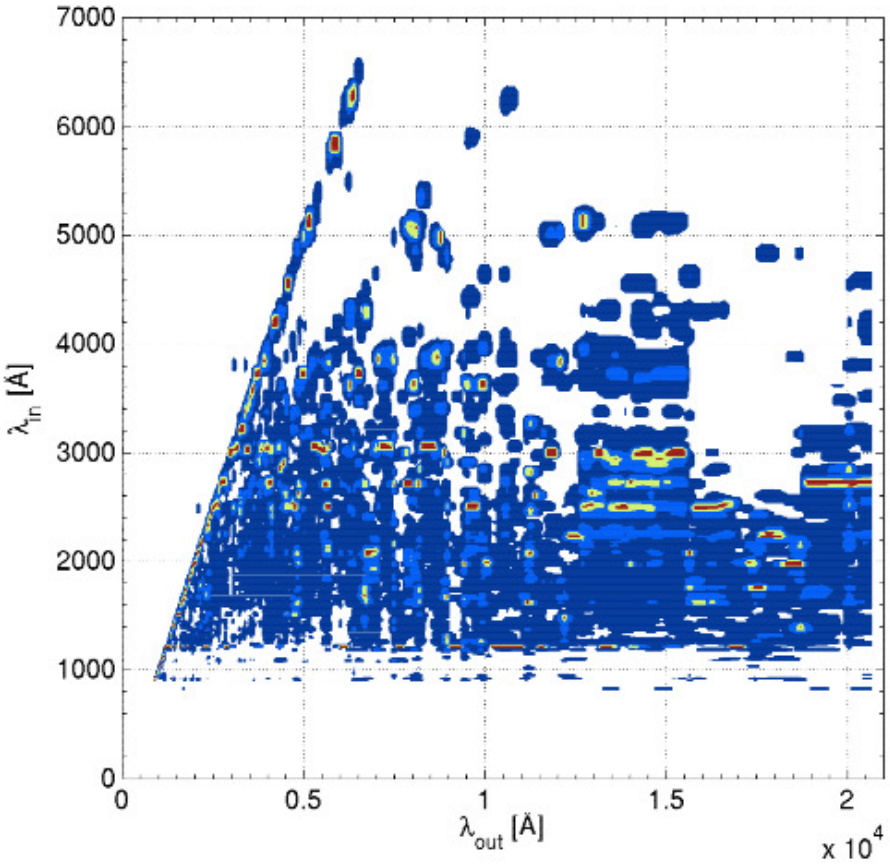

Figure 5: Fluorescence redistribution in a model of SN 1987A at an age of 8 years. From Jerkstrand et al 2011.

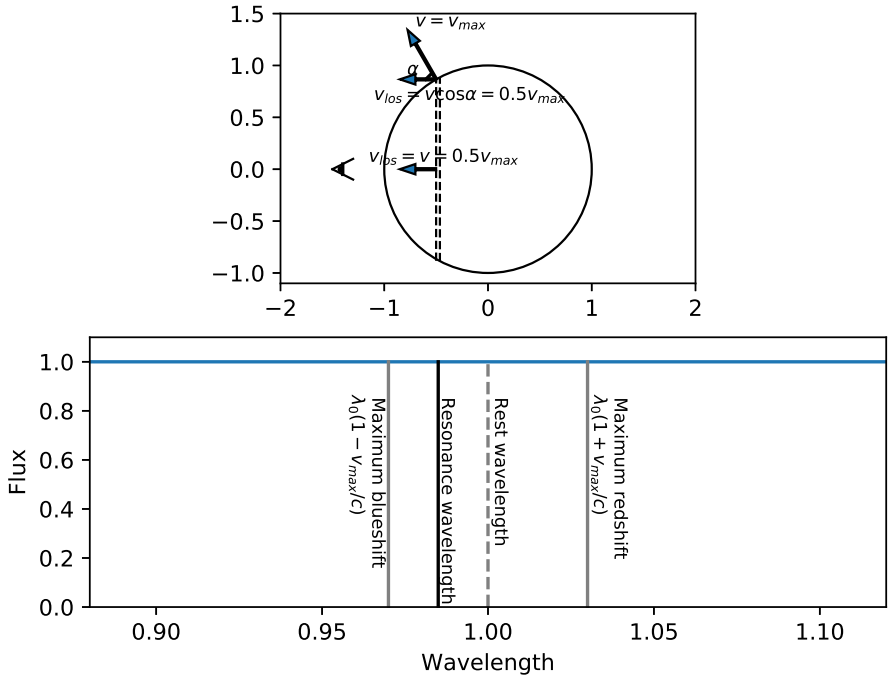

Figure 6: Illustration of how a sheet perpendicular to the LOS has constant LOS velocity, and therefore constant Doppler shift with respect to the observer. The bottom panel shows the corresponding wavelengths if each LOS point, in this example λ values are calculated for $v_{max}/c = 0.03$.

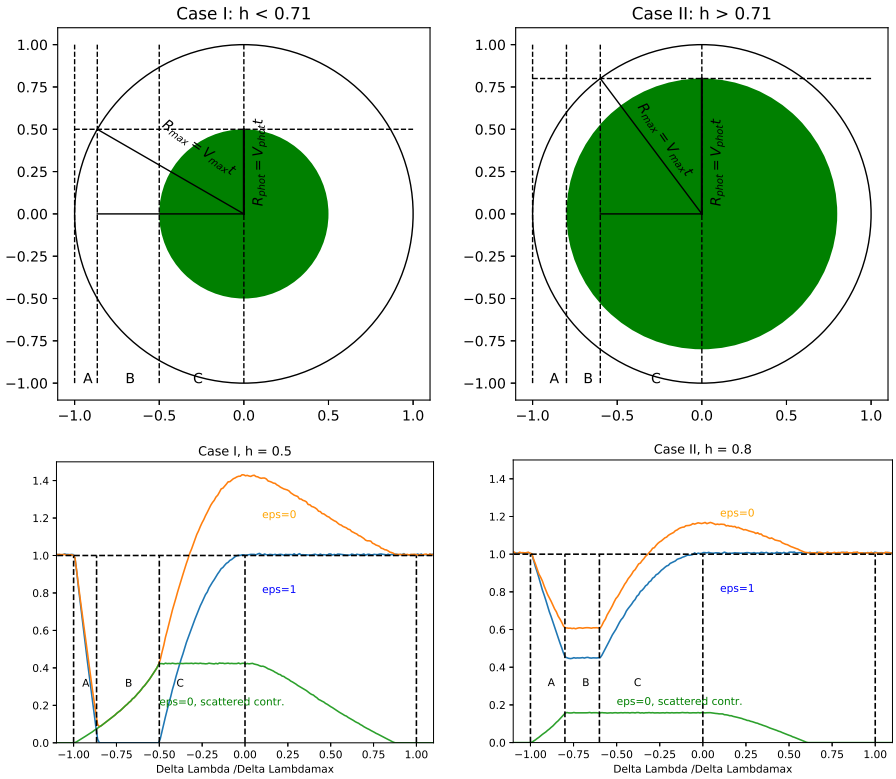

Figure 7: Geometry of P-Cygni line formation. The observer is towards the left.

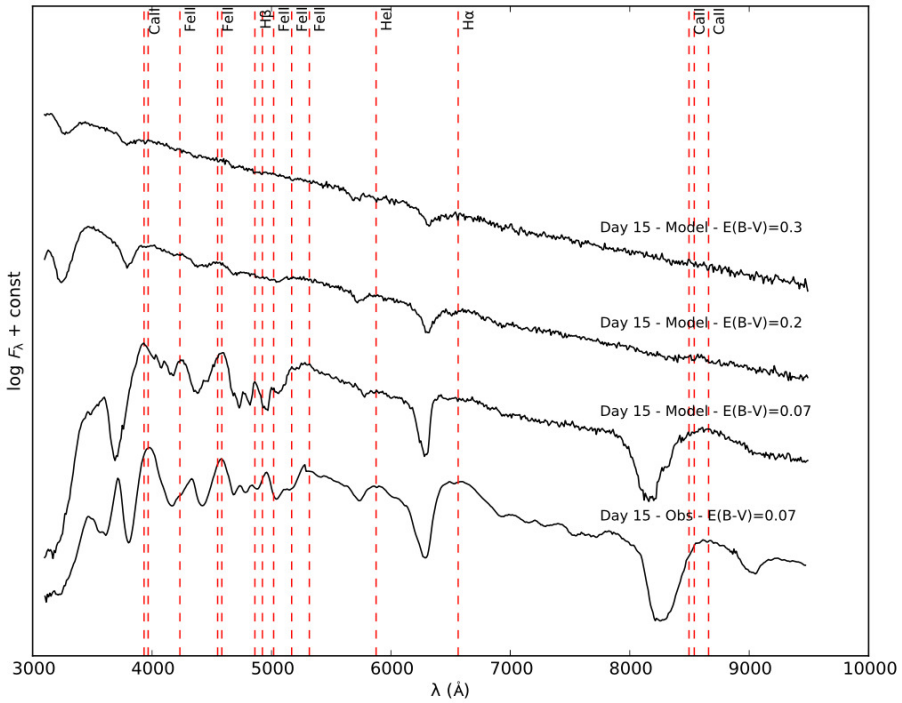

Figure 8: An observed SN spectrum showing P-Cygni lines (bottom curve, top ones are models). From Ergon+2014.

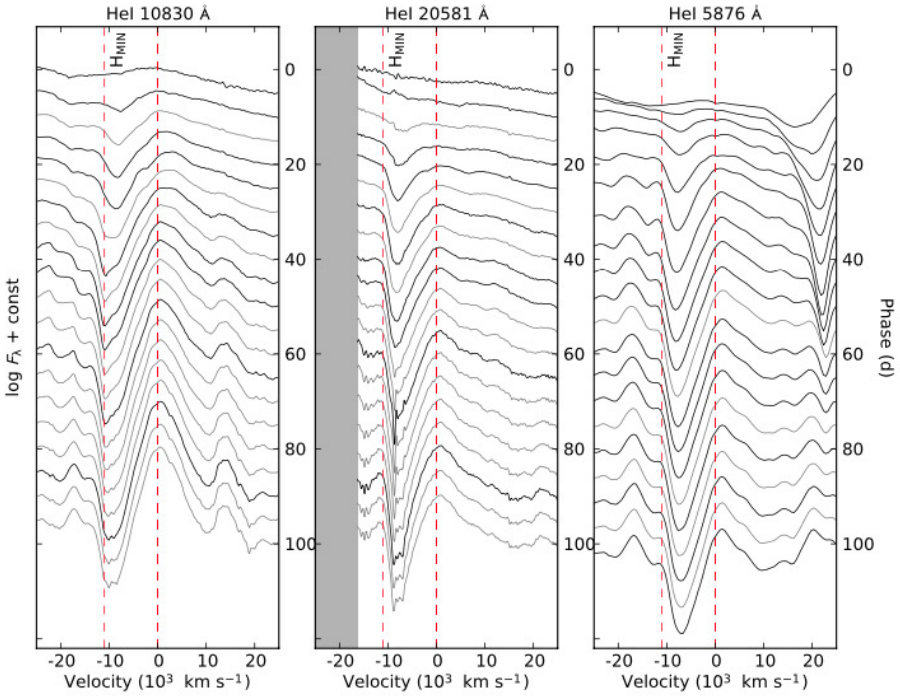

Figure 9: Observed evolution of He P-Cygni lines in a Type IIb SN. From Ergon et al 2014.

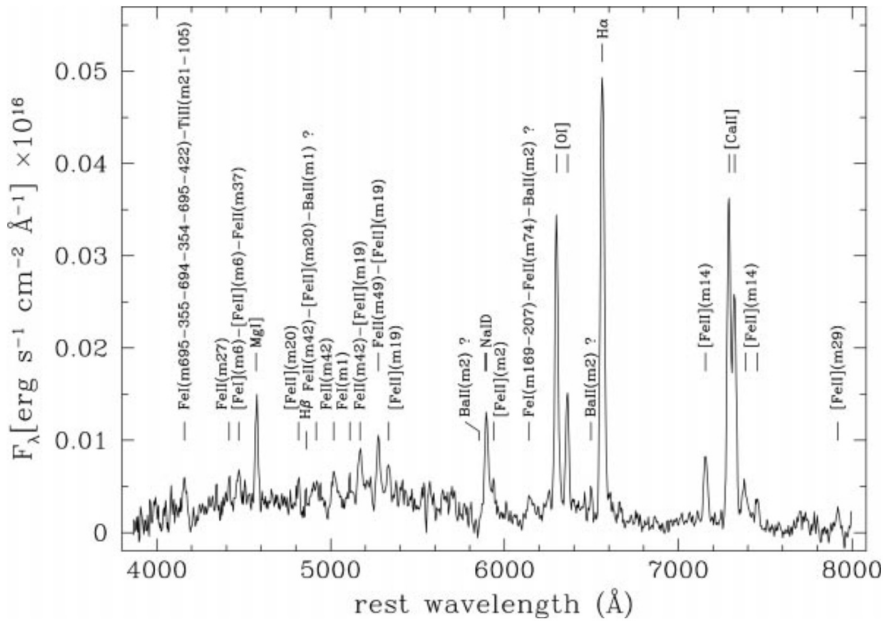

Figure 10: Example of an observed nebular spectrum from a low-velocity Type IIP SN, from Benetti et al. 2001. As the photosphere has disappeared there are no P-Cygni lines, instead the spectrum is made of emission lines, some of which are very prominent. Models show that what looks like "continuum" (e.g. between 6600-7000 Å) is in fact thousands of overlapping weaker emission lines.

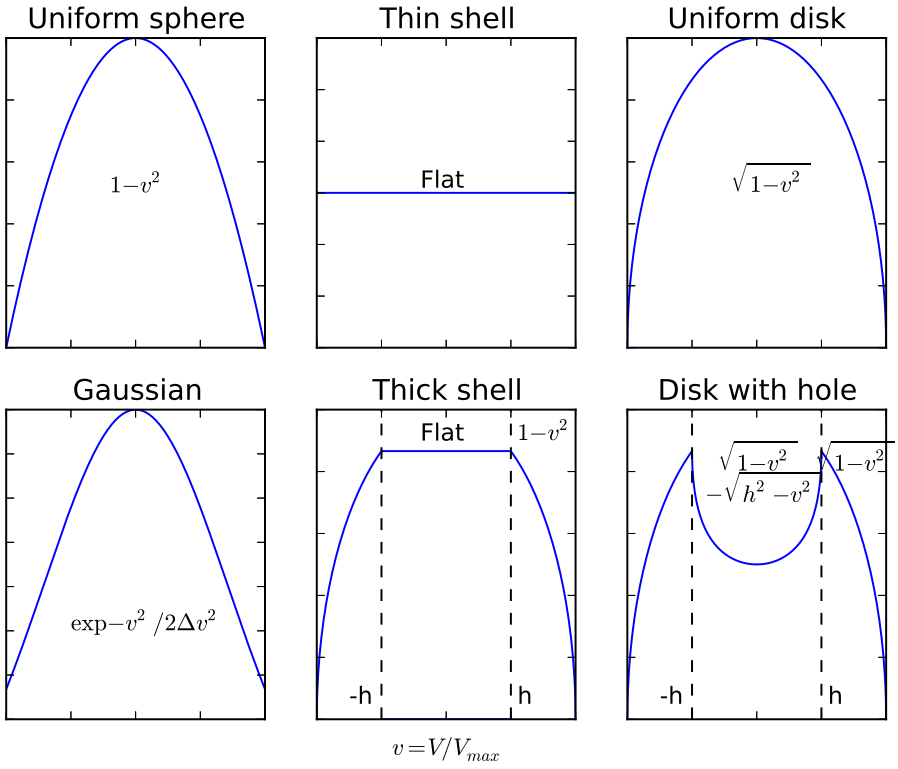

Figure 11: Nebular line profiles for 6 different cases. From Jerkstrand 2017 (Handbook of SNe).